Modulated Nonlinear Optical Responses and Charge Transfer Transition in Endohedral Fullerene Dimers Na@C60C60@F with n-Fold Covalent Bond (n = 1, 2, 5, and 6) and Long Range Ion Bo...

ARTICLE *in* THE JOURNAL OF PHYSICAL CHEMISTRY C · JUNE 2010

Impact Factor: 4.77 · DOI: 10.1021/jp9116479

Modulated Nonlinear Optical Responses and Charge Transfer Transition in Endohedral Fullerene Dimers Na@$C_{60}C_{60}$@F with *n*-Fold Covalent Bond ($n = 1, 2, 5$, and 6) and Long Range Ion Bond

Fang Ma, Zhi-Ru Li,* Zhong-Jun Zhou, Di Wu, Ying Li, Yin-Feng Wang, and Ze-Sheng Li*

State Key Laboratory of Theoretical and Computational Chemistry, Institute of Theoretical Chemistry, Jilin University, Changchun, 130023, China

Received: December 8, 2009; Revised Manuscript Received: April 12, 2010

Isomer structures of four endohedral fullerene dimers Na@$C_{60}C_{60}$@F with an *n*-fold bond ($n = 1, 2, 5$ and 6) are obtained for the first time by using density functional theory. The *n*-fold bond depends on the dimeric pattern between endohedral fullerenes Na@C_{60} and F@C_{60}. The pattern includes point−point ($n = 1$), side−side ($n = 2$), and face−face ($n = 5, 6$) mode. The four structures [**1** + **1**], [**2** + **2**], [**5** + **5**] and [**6** + **6**] have larger *n*-fold bond energies, as compared to that of the neutral π-$(C_{60})_2$ dimer. In addition, the electronic properties of the endohedral dimers are first investigated. The dimers exhibit a strong nonlinear optical (NLO) response: large static first hyperpolarizabilities. Moreover, the first hyperpolarizability depends on the dimeric pattern. The large first hyperpolarizabilitiy is up to 25 169 au for [**5** + **5**], which is almost 110 times larger than that of the NaF molecule (228 au). The great enhancement of the first hyperpolarizability relates to the geometric effect of expanding the Na···F distance from 1.980 for NaF to 6.355 Å for [**5** + **5**], which provides a novel strategy for enhancing the first hyperpolarizability by altering the molecular structure. It is also found that the crucial charge transfer transition depends on the dimeric pattern, and controlling the transition may be performed by modulating the dimeric pattern. This work may promote the study of new nanomaterials, including high-performance NLO materials, and enrich knowledge of chemical bonds (for example, multifold bond between cages) and long-range interaction between two trapped atoms in different cages.

Introduction

Endohedral fullerenes that encapsulate atoms or molecules inside the carbon cages have attracted increasing attention during recent decades.[1−3] The number of endohedral fullerenes has been constantly growing: for example, C_{60} endohedral complexes[4] with ions F^-, Ne, Na^+, or Mg^{2+} or molecules LiF or H_2[5] and larger carbon cages (such as C_{80} and C_{82}) with atomic clusters.[6] These endohedral fullerenes appear to be practical nanodevices. For example, the metallofullerene La_2@C_{80} can act as a field-effect transistor,[7] and the long spin lifetimes in N@C_{60} may be useful as a qubit in a quantum computer.[8]

For further development of the study on endohedral fullerenes, the endohedral fullerene dimer is an important object. The endohedral fullerene dimer presents a first step toward potential applications. However, endohedral fullerene dimers have scarcely been studied in both theory and experiment.[9] For the endohedral fullerene dimers, their knowledge on structure, interaction, and properties are very valuable. Here, the endohedral fullerene dimers Na@$C_{60}C_{60}$@F are investigated to obtain this knowledge.

Recent decades have witnessed progress in the design of nonlinear optical (NLO) materials[10] due to their potential use in optic device applications. In the search of NLO materials, the intramolecular charge-transfer system has been a successful motif for NLO materials design.[11] Na@$C_{60}C_{60}$@F may be a good candidate for an optical molecule with a large first hyperpolarizability due to its charge transfers and complex mutual polarizations. On the other hand, it is reported that the geometric effect (for example, the expanded covalent bond H···F distance by inserting Rg = He, Ar, and Kr) is obvious for enhancing first hyperpolarizability.[12] However, how to achieve the long-distance ionic bond Na^+···F^- enhancing the first hyperpolarizability target is still not reported. The endohedral fullerene dimers Na@$C_{60}C_{60}$@F may also be good candidates due to their long, expanded ionic bond Na^+···F^- by deftly trapping Na and F atoms separately into two C_{60} cages, which is obviously different from the idea of a reported expanded H···F distance.[12]

In this paper, we theoretically report the interesting structures of endohedral fullerene dimers, exhibit a dimeric pattern to form an *n*-fold covalent bond between two endohedral cages and a long-distance ionic bond between tapped atoms, and explore the relations between the dimeric pattern and first hyperpolarizability and the crucial charge transfer transition. The work enriches the knowledge of endohedral chemistry and may provide a new means for designing high-performance nonlinear optical (NLO) materials.

Calculation Details

Singlet optimized structures Na@$C_{60}C_{60}$@F; related structures Na@C_{60}, F@C_{60}, and neutral π-$(C_{60})_2$; and natural bond orbital (NBO)[13] charges are obtained by using the RB3LYP/6-31G method.[14] Triplet optimized structures and their energies for Na@$C_{60}C_{60}$@F are obtained at the UB3LYP/6-31G level. The vertical ionization potential (IP) values are calculated at the B3LYP/6-31G(d) level.

Considering the interaction between two endohedral fullerene monomers, the bond energy, E_b, between two endohedral fullerene monomers is calculated by using the B3LYP/6-311G(d) method. To correct the basis-set superposition error

* Address correspondence to either author. E-mail: (Z.R.L.) lzr@jlu.edu.cn; (Z.-S.L.)zeshengli@jlu.edu.cn.

10.1021/jp9116479
Published on Web 06/08/2010

in the bond energy calculation, the counterpoise (CP)[15] correction was used. The E_b is the difference between the energy of the endohedral complex (AB) and the sum of the energies of the monomers (A, B), as illustrated by the following formula:

$$E_b = E_A(X_{AB}) + E_B(X_{AB}) - E_{AB}(X_{AB}) \quad (1)$$

The same basis set, X_{AB}, is used for both the monomer and endohedral complex.

With regard to the calculation of the first hyperpolarizabilities of these large systems in the present study, choosing a proper method is important. The B3LYP method has been reported to overestimate the (hyper)polarizabilities for some large systems.[16] The MP2 method is more reliable than B3LYP in the (hyper)-polarizability calculations, but it is very costly for these large systems. A new density functional, a Coulomb-attenuated hybrid exchange-correlation functional (CAM-B3LYP),[17,18] has recently been developed specifically to overcome these limitations of the traditional density functional, and it has been shown to properly predict the molecular properties of charge-transfer processes.[19−21] In the current paper, the static first hyperpolarizabilities are evaluated by a finite field approach at the CAM-B3LYP level. The basis sets employed are 6-31G(d) for the C atoms and the 6-311+G(d) for trapped atoms F and Na. Champagne, Nakano, and co-workers pointed out that for a medium-size system, the BHandHLYP method can also reproduce the (hyper)polarizability values from the more sophisticated CCSD(T).[22,23] In our previous investigation, we found that the BHandHLYP value is close to the MP2 for the first hyperpolarizabilities calculated.[24] Moreover, a new hybrid meta exchange-correlation functional M05-2X presented by Truhlar[25] is also employed to evaluate the static first hyperpolarizabilities for large dimers. The results of BHandHLYP and M05-2X are close to those of CAM-B3LYP.

The static first hyperpolarizability is noted as

$$\beta_0 = (\beta_x^2 + \beta_y^2 + \beta_z^2)^{1/2} \quad (2)$$

where

$$\beta_i = \frac{3}{5}(\beta_{iii} + \beta_{ijj} + \beta_{ikk}) \qquad i,j,k = x,y,z$$

The frequency-dependent NLO properties of the four endohedral fullerene dimers are evaluated by the coupled-perturbed Hartree−Fock (CPHF) method.[26] The basis sets employed are 6-311+G(d) for trapped atoms and the 6-31G(d) basis set for C atoms.

The frequency dependent β is noted as

$$\bar{\beta}(\omega) = (\beta_x^2 + \beta_y^2 + \beta_z^2)^{1/2} \quad (3)$$

where

$$\beta_i = \frac{1}{5}[2\beta_{jji}(-2\omega;\omega,\omega) + \beta_{ijj}(-2\omega;\omega,\omega)] \qquad i,j = x,y,z$$

for the second harmonic generation (SHG) and

$$\beta_i = \frac{1}{5}[\beta_{jji}(-\omega;\omega,0) + 2\beta_{jij}(-\omega;\omega,0)] \qquad i,j = x,y,z$$

for the electro-optical Pokcets effect (EOPE).

In addition, the DFT frequency-dependent β is estimated by using the multiplicative approximation[27]

$$\beta(\omega)^{DFT} \cong \beta(\omega)^{HF}\beta(0)^{DFT}/\beta(0)^{HF} \quad (4)$$

All calculations are carried out by using the Gaussian03 program package,[28] except that the calculations for CAM-B3LYP are performed by the Gaussian09 program package.[29]

Results and Discussions

A. Geometrical Characteristics and Stability. In the dimeric pattern of Na@$C_{60}C_{60}$@F, four possible modes connecting two cages can arise. (i) The point−point mode forms a [**1** + **1**] dimer with a 1-fold C−C bond between C_{60} cages; (ii) the side−side mode forms a [**2** + **2**] dimer with a 2-fold bond; (iii) the face−face mode between two pentagonal rings forms a [**5** + **5**] dimer with a 5-fold bond; and (iv) the face−face mode between two hexagonal rings forms [**6** + **6**] dimer with a 6-fold bond. The optimized structures of the four dimers ([**1** + **1**], [**2** + **2**], [**5** + **5**], and [**6** + **6**]) are obtained. For the optimized structures, the singlet structure has lower energy than the corresponding triplet one (see Table S1 in the Supporting Information), so the ground state is the singlet. The total energies for each singlet structure are also given in Table S1. Here, the ground state structures are shown in Figure 1; the geometrical parameters are collected in Table 1.

In Figure 1, particularly for the [**1** + **1**], the 1-fold C−C bond length (1.583 Å) is shorter than that in the ó-$(C_{60}^-)_2$ dimer (1.598 Å),[30] due to ions inside the cages, but longer than that for the normal C−C bond between sp^3 carbons (1.541 Å).[31] In [**2** + **2**], the 2-fold C−C bond between Na@C_{60} and F@C_{60} is two intercage C−C bond of 1.611 Å lengths (see Table 1), which is obviously longer than those in the neutral π-$(C_{60})_2$ dimer (1.575 Å),[32] and also longer than those in the π-$(C_{60}^-)_2$ dimer (1.581 Å).[33]The 5-fold C−C bond length is 1.608 Å in [**5** + **5**], which is slightly shorter than those in [**2** + **2**] and shorter than the 6-fold C−C bond lengths of 1.617 Å in [**6** + **6**]. Moreover, from Table 1, it is found that $n = 1$ is much shorter than $n = 2$, 5, and 6 for the *n*-fold C−C bond length.

From Figure 1, the encapsulated Na and F atoms obviously depart from the center of the cage. As shown in Table 1, the off-center distances of the F atoms are in 1.105−1.548 Å in endohedral fullerene dimers Na@$C_{60}C_{60}$@F, which are obviously larger than that in the endohedral fullerene F@C_{60} monomer (0.344 Å). The off-center distances of Na atoms are 0.480−1.116 Å in the dimers Na@$C_{60}C_{60}$@F, which are larger than that in the endohedral fullerene Na@C_{60} monomer (0.346 Å). These indicate that the dimerization of endohedral cages with oppositely charged ions enhances the off-center distance of the trapped atom, which relates to the attraction between Na and F.

From Table 1, the charges of the F atoms in endohedral fullerene dimers Na@$C_{60}C_{60}$@F are −0.445 to about −0.844, which is larger than that in the eendohedral fullerene F@C_{60} (−0.384); all the charges of Na atoms are 0.836−0.876, which is also much larger than that in Na@C_{60} (0.534). These show that the dimerization of the endohedral cages obviously enhance the charges of F and Na inside the cages. Moreover, it is interesting that the charge transfers between cage and cage and

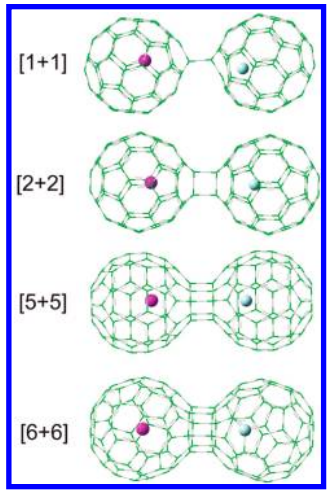

Figure 1. Optimized structures of endohedral fullerene dimers $Na@C_{60}C_{60}@F$.

trapped atom relate to the dimeric pattern (*n*-fold bond). The order of the $Na@C_{60}$ charges ($q_{Na@C60}$) is -0.071 ($n = 5$) < 0.018 ($n = 1$) ≪ 0.370 ($n = 6$) < 0.771 ($n = 2$), which shows that the charge transfer between $Na@C_{60}$ and $C_{60}@F$ is small for the dimers with odd *n* ($n = 1, 5$) but large for the dimers with odd *n* ($n = 2, 6$). Comparing the charges between the Na and C_{60} cage in the $Na@C_{60}$ cage, it is found that the charge transfers occur mainly between the cage and trapped Na for $n = 1$ and 5 because the q_{Na} is close to the absolute value of the C_{60} cage; but the charge transfers are long distance and mainly between $Na@C_{60}$ and $C_{60}@F$ from Na to F for $n = 2$ and 6, because the q_{Na} is much larger than the absolute value of the C_{60} cage.

On the other hand, the endohedral fullerene can be considered as a combination of a positively charged nucleus inside and a negatively charged cage outside, or a negatively charged nucleus inside and a positively charged cage outside.[7] Then, in endohedral fullerene dimers $Na@C_{60}C_{60}@F$, there exist not only covalent interactions between two cages but also interesting and complex electrostatic interactions among monomers, particularly long-distance electrostatic interactions between the trapped cation and anion. Recently, Petek et al pointed out that $Li@C_{60}$ can exhibit "superatom" character.[34] Hence, the endohedral fullerenes dimers $Na@C_{60}C_{60}@F$ may be consided as supermolecule salts, in which there exists the *n*-fold covalent bond between two cages and the long distance ionic bond between the cation and anion inside different cages.

As shown in Table 1, owing to the formation of the covalent bond, the endohedral fullerene dimers $Na@C_{60}C_{60}@F$ have large bond energies, E_b, between endohedral fullerene monomers within the range of 64.17−114.24 kcal/mol that are larger than that in the reported neutral π-$(C_{60})_2$ dimer (52.01 kcal/mol) by using the same method. This proves the stability of these endohedral fullerene dimers. We also note that the vertical IP values of endohedral fullerene dimers $Na@C_{60}C_{60}@F$ (20.683−21.032 eV) are about three times larger than that of $Na@C_{60}$ or $F@C_{60}$. It shows that the reducibility of the endohedral fullerene dimers is far weaker than that of endohedral fullerene monomers $Na@C_{60}$ and $F@C_{60}$, which indicates that the endohedral fullerene dimers have large stability. This provides a possible approach to increase the stability of a C_{60} polymer by putting the cation and anion inside different cages.

B. The Electronic Properties of Endohedral Fullerene Dimers. In this work, the electronic properties are calculated by a new density functional, a Coulomb-attenuated hybrid exchange-correlation functional (CAM-B3LYP). From Table 2, it can be seen that the electronic properties in the ground state depend on the dimeric pattern for the endohedral fullerene dimers with an *n*-fold bond. The order of the dipole moment, μ, values is 1.144 ([**5** + **5**]) < 2.114 ([**1** + **1**]) < 5.297 ([**6** + **6**]) < 11.063 au ([**2** + **2**]). It is shown that the μ values of $n = 2$ and 6 are much larger than those of $n = 1$ and 5. For odd or even *n*, the small *n* relates to the large μ value for the dimers. The relationships between μ and $q_{Na@C60}$ and the dimeric pattern are shown in Figure S1 in the Supporting Information. The order of the polarizability α_0 values is 1013 ([**1** + **1**]) < 1026 ([**6** + **6**]) < 1038([**2** + **2**]) < 1108 au ([**5** + **5**]). The α_0 value increases with increasing *n*, except for ([**6** + **6**]).

Here, we focus on the first hyperpolarizability β_0. When comparing with endohedral fullerenes $Na@C_{60}$ (710 au) and $F@C_{60}$ (2699 au), it is found that the dimerization of the two endohedral cages dramatically enhances first hyperpolarizability (2361−25169 au). Table 2 shows that the order of the β_0 values is 2361 ([**1** + **1**]) < 5405 ([**6** + **6**]) < 11779 ([**2** + **2**]) < 25169 au ([**5** + **5**]), which is similar to the order of the α_0 values. The β_0 values increases with increasing the *n*, except for ([**6** + **6**]). The largest β_0 for [**5** + **5**] ($Na@C_{60}C_{60}@F$ with 5-fold bond) is up to 25 169 au, which is almost 110 times larger than that of NaF (228 au). Why are the β_0 values of $Na@C_{60}C_{60}@F$ much larger than that of NaF? In $Na@C_{60}C_{60}@F$, the Na atom is trapped in one cage, and the F atom is trapped in another cage. The Na···F distances (6.355−7.058 Å) are much longer than Na−F of 1.980 Å. From the view of the molecular structure, the geometric effect of the increasing Na···F distance brought by ably trapping separately Na and F atoms in two C_{60} cages is an important factor for greatly enhancing first hyperpolarizability. This provides a novel strategy for enhancing the first hyperpolarizability by altering the molecular structure. In fact, the dimerization of the two endohedral cages $Na@C_{60}$ and $F@C_{60}$ forms not only an *n*-fold covalent bond between the cages, but also a long-distance $Na^+\cdots F^-$ interaction, which leads to interendohedral cage polarization, strengthens the

TABLE 1: The Connected Bond Length between Cages (C−C, in Å), the Off-Center Distances of F and Na Atoms (d_F and d_{Na}, in Å), the Distances between F and Na (F···Na, Å), NBO Charges (the Values in the Parentheses for C_{60} Cage), Bond Energies E_b (Kal/mol) between Two Endohedral Fullerenes, and Ionization Potential Values (eV)

	C−C	d_F	d_{Na}	F···Na	q_F	q_{Na}	$q_{Na@C60}$	$q_{F@C60}$	E_b	IP
[**1** + **1**]	1.583	1.548	0.936	6.960	−0.445	0.865	0.018 (−0.847)	−0.018 (0.427)	114.24	21.032
[**2** + **2**]	1.611	1.105	0.945	7.058	−0.844	0.863	0.771 (−0.092)	−0.771 (0.073)	113.02	20.747
[**5** + **5**]	1.608	1.355	1.116	6.355	−0.682	0.876	−0.071 (−0.947)	0.071 (0.753)	64.17	20.683
[**6** + **6**]	1.617	1.385	0.480	6.958	−0.662	0.836	0.370 (−0.486)	−0.370 (0.292)	104.66	20.831
C_{60}-C_{60}[a]	1.575[b]								52.01	
$F@C_{60}$		0.344			−0.384					7.616
$Na@C_{60}$			0.346			0.534				5.650

[a] C_{60}-C_{60} is the neutral π-$(C_{60})_2$ dimer. [b] Ref 32.

TABLE 2: Dipole Moment, μ (au); Polarizability, α_0 (au); Static First Hyperpolarizability, β_0 (au); Transition Energy, E_{n0} (eV); and Crucial Transitions

	[1 + 1]	[2 + 2]	[5 + 5]	[6 + 6]	NaF[a]
ν	2.114	11.063	1.144	5.297	3.306
α_0	1013	1026	1108	1038	9
β_{zzz}	−2333	−10301	−24883	6024	−257
β_0[b]	2361	11779	25169	5405	228
	2724	16056	30557	5397	
	2498	13339	32765	5563	
E_{n0}	2.023	1.651	1.289	1.839	2.584
crucial transition	0.61 (HOMO → LUMO-4)	0.36 (HOMO-5 → LUMO+1)	0.69 (HOMO → LUMO +1)	0.40 (HOMO-5 → LUMO)	0.70 (HOMO → LUMO+1)

[a] The results of NaF are obtained at the CCSD/6-311+G(3df) level. [b] The values of β_0 in the first line, at the CAM-B3LYP level; in the second line, at BHandHLYP level; and in the third line, at the M05-2X level.

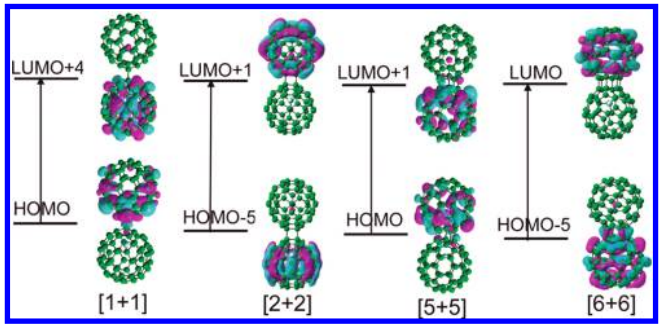

Figure 2. Crucial transitions depending on the dimeric pattern.

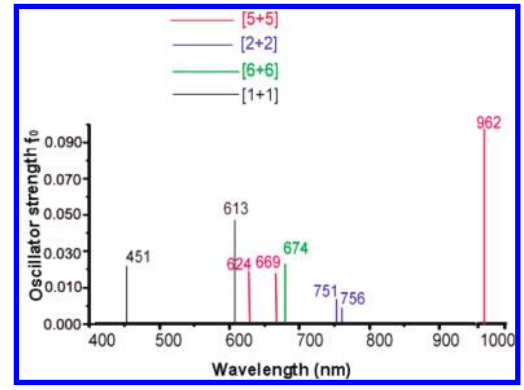

Figure 3. The linear absorption spectral of the endohedral fullerene dimers Na@$C_{60}C_{60}$@F.

polarization between the cage and the tapped atom, and especially brings about a strong polarization between the trapped atoms Na and F. The bonding interaction and polarizations lead to the variety of electronic structure, which brings about a large first hyperpolarizability.

It is interesting to compare the large β_0 values of the other systems. Compared with the reported electrides, the β_0 values of the endohedral fullerene dimers are close to that of the electride Li@calix[4]pyrrole (7326 au) and that of the electride $Li_n-H-(CF_2-CH_2)_3-H$ (n = 1, 2) (3694−76978au).[35] Furthermore, the β_0 value of the [**5** + **5**] (25 169 au) is close to that of the organometallic system Ru(*trans*-4,4′-diethylaminostyryl-2,2′-bipyridine)$_3^{2+}$ (31 123 au) and *cis*-[RuII$(NH_3)_4$(2-PymQ$^+$)$_2$][PF_6]$_4$ (34 487 au).[36]

The TD-DFT calculations are carried out to get the crucial transitions of these four dimers, and the crucial transitions with the largest oscillator strength and lower transition energy are illustrated in Figure 2. The order of the transition energy E_{n0} is 2.023 ([**1** + **1**]) < 1.839 ([**6** + **6**]) < 1.651 eV ([**2** + **2**]) < 1.289 ([**5** + **5**]) (see Table 2). It is found that the order of E_{n0} is consistent with the order of β_0, which shows that the transition energy is one controlling factor for β_0.

Notice that the crucial transition is interesting for these four dimers. The transition mode depends on the *n*-fold bond. From Figure 2, the crucial transitions for these four dimers are from one endohedral C_{60} cage to another, but the directions of transitions are different. For n = 1 and 5 ([**1** + **1**] and [**5** + **5**]), their directions are from endohedral fullerenes Na@C_{60} to F@C_{60}, whereas for n = 2 and 6 [**2** + **2**] and [**6** + **6**], their directions are from endohedral fullerenes F@C_{60} to Na@C_{60}. In the endohedral fullerene dimers, the crucial transitions are local and charge transfer transitions. Hence, controlling the transition mode may be performed by modulating the dimeric pattern, which may have potential applications in nanoelectronics.

The molecular hyperpolarizability relates to its electronic spectrum. To show the change trend of the absorption spectra for these endohedral fullerene dimers, the calculated linear absorption spectra of four dimers are shown in Figure 3. There exist dramatic differences in those four spectra. Interestingly, for [**5** + **5**], the strongest peak is mainly at 962 nm in the infrared region, whereas for [**1** + **1**], [**2** + **2**], and [**6** + **6**], the strongest peaks are 612, 751, and 674 nm in the visible region, respectively. Compared with the absorption strength of [**2** + **2**], the absorption strength of [**6** + **6**] slightly increases, but the absorption strengths of [**5** + **5**] and [**1** + **1**] obviously increase. Note that in the four dimers, the strongest peak of the dimer [**5** + **5**] has the largest wavelength and the strongest strength. These results exhibit that the absorption spectra depends on the dimeric pattern.

C. Frequency-Dependent NLO Properties. The frequency dependent properties have been computed by using the coupled perturbed Hartree−Fock theory CPHF. Table 3 lists the CPHF and estimated DFT (CAM-B3LYP) frequency-dependent values: the second harmonic generation (SHG) $\beta(-2\omega; \omega, \omega)$ and the electro-optical Pokcets effect (EOPE) $\beta(-\omega; \omega, 0)$ at ω = 0.0000, 0.0050, 0.0100, and 0.0239 au.

It is found that the effects of electron correlation on β_0 are very important for the dimers (see Table 3). To understand the contributions of electron correlation, the β_0 values of the four $Na^+\cdots F^-$ model systems are calculated at the HF and CAM-B3LYP level (see Table S2 in the Supporting Information). The distance of Na···F in the model system is taken from the equilibrium geometry of the corresponding endohedral fullerene dimer. By comparing HF with CAM-B3LYP results, it is seen that the results show that the contributions of electron correlation on β_0 values are similar (96.0−96.8%) for the four $Na^+\cdots F^-$ model systems, so the change of the contributions of electron correlation on the β_0 in four model systems $Na^+\cdots F^-$ is small. However, in Table S2, the contributions of the electron correlation in the four dimers are 27.0%, 79.0%, 87.3%, and 69.5%, respectively, which shows the obvious change of electron

TABLE 3: Estimated DFT (CAM-B3LYP) and the CPHF Values of Frequency-Dependent Hyperpolarizabilities (au)[a] and Electron Correlation Contribution (η)

	frequency (au)	$\beta(-2\omega; \omega, \omega)$	$\beta(-\omega; \omega, 0)$	η^b (%)
[**1** + **1**]	0.0000	2361 (1735)		27.0
	0.0050	2382 (1751)	2368 (1740)	
	0.0100	2438 (1791)	2390 (1756)	
	0.0239	2908 (2137)	2535 (1863)	
[**2** + **2**]	0.0000	11779 (2473)		79.0
	0.0050	11826 (2483)	11784 (2474)	
	0.0100	12021 (2524)	11845 (2487)	
	0.0239	13431 (2820)	12269 (2576)	
[**5** + **5**]	0.0000	25169 (3191)		87.3
	0.0050	27977 (3547)	27510 (3488)	
	0.0100	30207 (3830)	28228 (3579)	
	0.0239	53884 (6832)	33804 (4286)	
[**6** + **6**]	0.0000	5405 (1648)		69.5
	0.0050	5428 (1655)	5415 (1651)	
	0.0100	5504 (1678)	5442 (1659)	
	0.0239	6016 (1834)	5602 (1708)	

[a] The CPHF values are in parentheses. [b] η = ([CAM-B3LYP]-HF)/CAM-B3LYP.

correlation on the β_0. Thus, the changes of the electron correlation effects on the β_0 for the dimers are maybe due to the difference in the dimeric pattern between two cages.

For dimers [**2** + **2**] and [**6** + **6**] with even n fold bonds, compared with the corresponding β_0 values, the estimated DFT frequency-dependent values $\beta(-2\omega; \omega, \omega)$ and $\beta(-\omega; \omega, 0)$ of [**2** + **2**] are 13 431 and 12 269 au, increasing by ~14% and 4% at $\omega = 0.0239$ au, respectively. The $\beta(-2\omega; \omega, \omega)$ and $\beta(-\omega; \omega, 0)$ of [**6** + **6**] are 6016 and 5602 au, increasing by ~11% and 4% at $\omega = 0.0239$ au, respectively. Those show that the frequency-dependent effect is weak for [**2** + **2**] and [**6** + **6**].

For the dimer [**1** + **1**], compared with the β_0 value of 2361 au, the estimated DFT frequency-dependent values, $\beta(-2\omega; \omega, \omega)$ and $\beta(-\omega; \omega, 0)$ are 2908 and 2535 au, increasing by about 23% and 7% at $\omega = 0.0239$ au, respectively. It shows that the frequency-dependent effect is slightly stronger than those for [**2** + **2**] and [**6** + **6**].

Note that the dispersion effect on the dimer [**5** + **5**] is very strong. Compared with the large β_0 value of 25 169 au, the estimated DFT frequency-dependent values $\beta(-2\omega; \omega, \omega)$ and $\beta(-\omega; \omega, 0)$ are 53884 and 33804 au, increasing by about 114% and 34% at $\omega = 0.0239$ au, respectively. Obviously, comparing the other three dimers, the frequency-dependent effect is the most obvious for [**5** + **5**].

Conclusion

In this paper, four structures of endohedral fullerene dimers $Na@C_{60}C_{60}@F$ have been obtained for the first time. In these structures, there exists the n-fold covalent bond between two cages and a long-distance ionic bond between the cation and anion inside the different cages. Especially, the first hyperpolarizabilities of the $Na@C_{60}C_{60}@F$ were first investigated. The first hyperpolarizability depends on the dimeric pattern. The largest first hyperpolarizabilitiy is up to 25 169 au for [**5** + **5**], which is almost 110 times larger than that of NaF molecule (228 au). This paper provides a novel strategy for enhancing the first hyperpolarizability by forming a long-distance ion pair. We expect that this work will promote the study of endohedral fullerenes and potential candidate high-performance NLO materials and note that the crucial transition can be controlled by modulating the dimeric pattern, which may have potential applications in nanoelectronics.

Acknowledgment. This work is supported by the National Natural Science Foundation of China (No. 20773046).

Supporting Information Available: Complete refs 28 and 29, relative energies for singlet and triplet optimized structures, relationship between $q_{Na@C60}$ and dipole moment μ, the effects of electron correlation of the model systems $Na^+\cdots F^-$ and four dimers, and Cartesian coordinates for the singlet optimized endohedral fullerene dimers $Na@C_{60}C_{60}@F$. This material is available free of charge via the Internet at http://pubs.acs.org.

References and Notes

(1) Bethune, D. S.; Johnson, R. D.; Salem, J. R.; De Vries, M. S.; Yannoni, C. S. *Nature* **1993**, *366*, 123.
(2) Shinohara, H. *Rep. Prog. Phys.* **2000**, *63*, 843.
(3) Dunsch, L.; Yang, S. *Phys. Chem. Chem. Phys.* **2007**, *9*, 3067.
(4) Cioslowski, J.; Fleischmann, E. D. *J. Chem. Phys.* **1991**, *94*, 3730.
(5) (a) Hu, Y. H.; Ruckenstein, E. *J. Am. Chem. Soc.* **2005**, *127*, 11277. (b) Komatsu, K.; Murata, M.; Murata, Y. *Science* **2005**, *307*, 238.
(6) (a) Stevenson, S.; Rice, G.; Glass, T.; Harich, K.; Cromer, F.; Jordan, M. R.; Craft, J.; Hadju, E.; Bible, R.; Olmstead, M. M.; Maitra, K.; Fisher, A. J.; Balch, A. L.; Dorn, H. C. *Nature* **1999**, *401*, 55–57. (b) Wang, C. R.; Kai, T.; Tomiyama, T.; Yoshida, T.; Kobayashi, Y.; Nishibori, E.; Takata, M.; Sakata, M.; Shinohara, H. *Angew. Chem., Int. Ed.* **2001**, *40*, 397–399. (c) Iiduka, Y.; Wakahara, T.; Nakajima, K.; Nakahodo, T.; Tsuchiya, T.; Maeda, Y.; Akasaka, T.; Yoza, K.; Liu, M. T. H.; Mizorogi, N.; Nagase, S. *Angew. Chem., Int. Ed.* **2007**, *46*, 5562–5564. (d) Iiduka, Y.; Wakahara, T.; Nakahodo, T.; Tsuchiya, T.; Sakuraba, A.; Maeda, Y.; Akasaka, T.; Yoza, K.; Horn, E.; Kato, T.; Liu, M. T. H.; Mizorogi, N.; Kobayashi, K. *J. Am. Chem. Soc.* **2005**, *127*, 12500–12501. (e) Stevenson, S.; Mackey, M. A.; Stuart, M. A.; Phillips, J. P.; Easterling, M. L.; Chancellor, C. J.; Olmstead, M. M.; Balch, A. L. *J. Am. Chem. Soc.* **2008**, *130*, 11844–11845.
(7) Kobayashi, S.; Mori, S.; Iida, S.; Ando, H.; Takenobu, T.; Taguchi, Y.; Fujiwara, A.; Taninaka, A.; Shinohara, H.; Iwasa, Y. *J. Am. Chem. Soc.* **2003**, *125*, 8116.
(8) (a) Harneit, W. *Phys. Rev. A* **2002**, *65*, 032322. (b) Benjamin, S. C.; Ardavan, A.; Briggs, G. A. D.; Britz, D. A.; Gunlycke, D.; Jefferson, J.; Jones, M. A. G.; Leigh, D. F.; Lovett, B. W.; Khlobystov, A. N.; Lyon, S.; Morton, J. J. L.; Porfyrakis, K.; Sambrook, M. R.; Tyryshkin, A. M. *J. Phys.: Condens. Matter* **2006**, *18*, S867.
(9) Feng, L.; Tsuchiya, T.; Wakahara, T.; Nakahodo, T.; Piao, Q.; Maeda, Y.; Akasaka, T.; Kato, T.; Yoza, K.; Horn, E.; Mizorogi, N.; Nagase, S. *J. Am. Chem. Soc.* **2006**, *128*, 5990.
(10) (a) Eaton, D. F. *Science* **1991**, *253*, 281–287. (b) Geskin, V. M.; Lambert, C.; Brédas, J.-L. *J. Am. Chem. Soc.* **2003**, *125*, 15651–15658. (c) Nakano, M.; Fujita, H.; Takahata, M.; Yamaguchi, K. *J. Am. Chem. Soc.* **2002**, *124*, 9648–9655. (d) Long, N. J.; Williams, C. K. *Angew. Chem., Int. Ed.* **2003**, *42*, 2586–2617. (e) Avramopoulos, A.; Reis, H.; Li, J.; Papadopoulos, M. G. *J. Am. Chem. Soc.* **2004**, *126*, 6179–6184. (f) Bouder, T. L.; Maury, O.; Bondon, A.; Costuas, K.; Amouyal, E.; Ledoux, I.; Zyss, J.; Le Bozec, H. *J. Am. Chem. Soc.* **2003**, *125*, 12284–12299. (g) Kirtman, B.; Champagne, B.; Bishop, D. M. *J. Am. Chem. Soc.* **2000**, *122*, 8007–8012. (h) Marder, S. R.; Torruellas, W. E.; Blanchard-Desce, M.; Ricci, V.; Stegeman, G. I.; Gilmour, S.; Brédas, J.-L.; Li, J.; Bublitz, G. U.; Boxer, S. G. *Science* **1997**, *276*, 1233. (i) Champagne, B.; Spassova, M.; Jadin, J.-B.; Kirtman, B. *J. Chem. Phys.* **2002**, *116*, 3935.
(11) (a) Bossi, A.; Licandro, E.; Maiorana, S.; Rigamonti, C.; Righetto, S.; Stephenson, G. R.; Spassova, M.; Botek, E.; Champagne, B. *J. Phys. Chem. C* **2008**, *112*, 7900. (b) Sanguinet, L.; Pozzo, J. L.; Rodriguez, V.; Adamietz, F.; Castet, F.; Ducasse, L.; Champagne, B. *J. Phys. Chem. B* **2005**, *109*, 11139. (c) Coe, B. J.; Harris, J. A.; Hall, J. J.; Brunschwig, B. S.; Hung, S. T.; Libaers, W.; Clays, K.; Coles, S. J.; Horton, P. N.; Light, M. E.; Hursthouse, M. B.; Garín, J.; Orduna, J. *Chem. Mater.* **2006**, *18*, 5907. (d) Nakano, M.; Kishi, R.; Ohta, S.; Takahashi, H.; Kubo, T.; Kamada, K.; Ohta, K.; Botek, E.; Champagne, B. *Phys. Rev. Lett.* **2007**, *99*, 033001. (e) Coe, B. J.; Harris, J. A.; Jones, L. A.; Brunschwig, B. S.; Song, K.; Clays, K.; Garín, J.; Orduna, J.; Coles, S. J.; Hursthouse, M. B. *J. Am. Chem. Soc.* **2005**, *127*, 4845. (f) Kang, H.; Facchetti, A.; Jiang, H.; Cariati, E.; Righetto, S.; Ugo, R.; Zuccaccia, C.; Macchioni, A.; Stern, C. L.; Liu, Z.; Ho, S.-T.; Brown, E. C.; Ratner, M. A.; Marks, T. J. *J. Am. Chem. Soc.* **2007**, *129*, 3267. (g) Nakano, M.; Ohta, S.; Tokushima, K.; Kishi., R.; Kubo, T.; Kamada, K.; Ohta, K.; Champagne, B.; Botek, E.; Takahashi, H. *Chem. Phys. Lett.* **2007**, *443*, 95. (h) Botek, E.; Spassova, M.; Champagne, B.; Asselberghs, I.; Persoons, A.; Clays, K. *Chem. Phys. Lett.* **2005**, *412*, 274.

(12) (a) Liu, Z. B.; Li, Z. R.; Zuo, M. H.; Li, Q. Z.; Ma, F.; Li, Z. J.; Chen, G. H.; Sun, C. C. *J. Chem. Phys.* **2009**, *131*, 044308. (b) Papadopoulos, M. G.; Avramopoulos, A. *AIP Conf. Proc.* **2007**, *963*, 316. (c) Avramopoulos, A.; Reis, H.; Li, J.; Papadopoulos, M. G. *J. Am. Chem. Soc.* **2004**, *126*, 6179. (d) Holka, F.; Avramopoulos, A.; Loboda, O.; Kellö, V.; Papadopoulos, M. G. *Chem. Phys. Lett.* **2009**, *472*, 185.

(13) (a) Reed, A. E.; Weinstock, R. B.; Weinhold, F. *J. Chem. Phys.* **1985**, *83*, 735. (b) Carpenter, J. E.; Weinhold, F. *J. Mol. Struct. (Theochem)* **1988**, *169*, 41.

(14) Lee, C.; Yang, W.; Parr, R. G. *Phys. Rev. B* **1988**, *37*, 785.

(15) (a) Boys, S. F.; Bernardi, F. *J. Mol. Phys.* **1970**, *19*, 553. (b) Turi, L.; Dannenberg, J. J. *J. Phys. Chem.* **1993**, *97*, 2488.

(16) Champagne, B.; Perpéte, E. A.; Jacquenmin, D.; van Gisbergen, S. J. A.; Baerends, E.-J.; Soubra-Ghaoui, C.; Robins, K. A. *J. Phys. Chem. A* **2000**, *104*, 4755–4763.

(17) Tawada, Y.; Tsuneda, T.; Yanagisawa, S.; Yanai, T.; Hirao, K. *J. Chem. Phys.* **2004**, *120*, 8425.

(18) Yanai, T.; Tew, D. P.; Handy, N. C. *Chem. Phys. Lett.* **2004**, *393*, 51.

(19) Peach, M. J. G.; Helgaker, T.; Salek, P.; Keal, T. W.; Lutnaes, O. B.; Tozer, D. J.; Handy, N. C. *Phys. Chem. Chem. Phys.* **2006**, *8*, 558.

(20) Kobayashi, R.; Amos, R. D. *Chem. Phys. Lett.* **2006**, *420*, 106.

(21) Cai, Z. L.; Crossley, M. J.; Reimers, J. R.; Kobayashi, R.; Amos, R. D. *J. Phys. Chem. B* **2006**, *110*, 15624–15632.

(22) Champagne, B.; Botek, E.; Nakano, M.; Nitta, T.; Yamaguchi, K. *J. Chem. Phys.* **2005**, *122*, 114315.

(23) Nakano, M.; Kishi, R.; Nitta, T.; Kubo, T.; Nakasuji, K.; Kamada, K.; Ohta, K.; Champagne, B.; Botek, E.; Yamaguchi, K. *J. Phys. Chem. A* **2005**, *109*, 885–89.

(24) (a) Wang, F. F.; Li, Z. R.; Wu, D.; Wang, Bi. Q.; Li, Y.; Li, Z. J.; Chen, W.; Yu, G. T.; Gu, F. L.; Aoki, Y. *J. Phys. Chem. B* **2008**, *112*, 1090–1094. (b) Chen, W.; Li, Z. R.; Wu, D.; Li, R. Y.; Sun, C. C. *J. Phys. Chem. B* **2005**, *109*, 601–608.

(25) Zhao, Y.; Schultz, N. E.; Truhlar, D. G. *J. Chem. Theory Comput.* **2006**, *2*, 364.

(26) (a) Dykstra, C. E.; Jasien, P. G. *Chem. Phys. Lett.* **1984**, *109*, 388. (b) Pulay, P. *J. Chem. Phys.* **1983**, *78*, 5043.

(27) (a) Dalskov, E. K.; Jensen, H. J. A.; Oddershede, J. *Mol. Phys.* **1997**, *12*, 3. (b) Jacquemin, D.; Quinet, O.; Champagne, B.; Andre, J. M. *J. Chem. Phys.* **2004**, *120*, 9401.

(28) Frisch, M. J.; *Gaussian 03, revision E.01*; Gaussian, Inc.: Wallingford, CT, 2004.

(29) Frisch, M. J.; *Gaussian 09, revision A.02*; Gaussian, Inc.: Wallingford, CT, 2009.

(30) Konarev, D. V.; Khasanov, S. S.; Otsuka, A.; Saito, G. *J. Am. Chem. Soc.* **2002**, *124*, 8520–8521.

(31) Kennard, O. In *CRC Handbook of Chemistry and Physics*; Weast, R. C., Ed.; CRC Press: Boca Raton, FL, 1987; p F106.

(32) (a) Wang, G. W.; Komatsu, K.; Murata, Y.; Shiro, M. *Nature* **1997**, *387*, 583–586. (b) Fujitsuka, M.; Luo, C.; Ito, O.; Murata, Y.; Komatsu, K. *J. Phys. Chem. A* **1999**, *103*, 7155–7160.

(33) Konarev, D. V.; Khasanov, S. S.; Otsuka, A.; Saito, G.; Lyubovskaya, R. N. *J. Am. Chem. Soc.* **2006**, *128*, 9292–9293.

(34) Feng, M.; Zhao, J.; Petek, H. *Science* **2008**, *320*, 359.

(35) (a) Chen, W.; Li, Z. R.; Wu, D.; Li, Y.; Sun, C. C.; Gu, F. L. *J. Am. Chem. Soc.* **2005**, *127*, 10977–10981. (b) Xu, H. L.; Li, Z. R.; Wu, D.; Wang, B. Q.; Li, Y.; Gu, F. L.; Aoki, Y. *J. Am. Chem. Soc.* **2007**, *129*, 2967–2970.

(36) (a) Vance, F. W.; Hupp, J. T. *J. Am. Chem. Soc.* **1999**, *121*, 4047–4053. (b) Coe, B. J.; Harris, J. A.; Jones, L. A.; Brunschwig, B. S.; Song, K.; Clays, K.; Garín, J.; Orduna, J.; Coles, S. J.; Hursthouse, M. B. *J. Am. Chem. Soc.* **2005**, *127*, 4845–4859.

JP9116479